Carbohydrate Research, 221 (1991) 95–121
Elsevier Science Publishers B.V., Amsterdam

N.m.r. and conformational analysis of the capsular polysaccharide from *Streptococcus pneumoniae* type 4

Christopher Jones*, Felicity Currie†, and Mark J. Forster‡
Laboratory of Molecular Structure, National Institute for Biological Standards and Control, Blanche Lane, South Mimms, Herts. EN6 3QG (Great Britain)

(Received February 6th, 1991; accepted for publication May 23rd, 1991)

ABSTRACT

The ^{1}H- and ^{13}C-n.m.r. data on the capsular polysaccharide (**1**) produced by *Streptococcus pneumoniae* type 4, the depyruvated polysaccharide (**2**), and a tetrasaccharide (**3a**) derived by Smith degradation of **2** were used as constraints on a computer-generated model of the conformation of **1** and to assess the effects of the pyruvic acetal substituent on the conformation. The dynamics of the polysaccharide systems and the influence of the pyruvic acetal were investigated using ^{13}C-n.m.r. relaxation measurements.

INTRODUCTION

A mixture of the purified capsular polysaccharides from several (14, 17, or 23 depending on the origin) of the 84 *Streptococcus pneumoniae* serotypes is used as a vaccine against pneumococcal pneumonia[1], and serum containing antibodies against a polysaccharide is bacteriocidal to that serotype. Many of these polysaccharides and similar antigenic polysaccharides carry non-carbohydrate substituents, of which *O*-acetyl groups and pyruvic acetals are the most common. These substituents influence the immunological specificity and patterns of immunological cross-reactivity. The polysaccharide from *S. pneumoniae* type 4 (S4, **1**) is a component of all three vaccines and has a pyruvated tetrasaccharide repeating unit[2]. The published[2a] structure of S4 has been revised on the basis of n.m.r. data[2b], which revealed a Gal-(1→3)-ManNAc linkage rather than the Gal-(1→4)-ManNAc linkage.

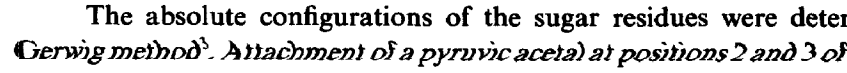

The absolute configurations of the sugar residues were determined[2a] by the Gerwig method[3]. Attachment of a pyruvic acetal at positions 2 and 3 of Gal is unique to S4 (although linkage at similar positions of β-GlcA is known[4]), the stereochemistry[2c] at C-2 of the pyruvic acetal is *S*, and treatment of S4 with dilute acid gave depyruvated S4, with the repeating unit **2**.

* To whom correspondence should be addressed.
† Present address: Xenova Ltd., 545 Ipswich Road, Slough, Berks. SL1 4EQ, Great Britain.
‡ Informatics Laboratory.

0008-6215/91/$ 03.50

→3)-β-D-ManNAc-(1→3)-α-L-FucNAc-(1→3)-α-D-GalNAc-(1→4)-α-D-Gal-(1→

2

Removal of the pyruvic acetal led to a decrease in viscosity of aqueous solutions and rendered the Gal residue susceptible to Smith degradation[5]. Hydrolysis of periodate-oxidised borohydride-reduced **2** with dilute acid gave a mixture of the tetrasaccharides[2a] **3a** and **3b**.

β-D-ManNAc-(1→3)-α-L-FucNAc-(1→3)-α-D-GalNAc-(1→O-R

3a R = 2-threitol

3b R =

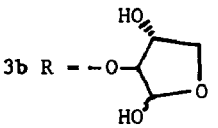

An understanding of the effects of non-carbohydrate substituents on the conformation and dynamics of these polysaccharides may provide a deeper insight into their immunological properties and so improve understanding of their clinical use. N.m.r.-derived distance constraints have been used to build computer models of these polysaccharides, from which n.m.r. data were simulated for testing against the experimental data.

The conformational analysis of polysaccharides is complicated by the paucity of inter-residue n.O.e.'s (and no n.O.e.'s to any residue apart from nearest neighbours). Energy calculations are generally less reliable than for peptides[6] and much more peripheral information from, for example, arguments on chemical shifts must be used to generate a trustworthy conformation.

EXPERIMENTAL

The general methods have been described[7]. The polysaccharide S4 was a gift from Merck, Sharp and Dohme Ltd. (Rahway, New Jersey) and was a sample of that used for the production of vaccine. High-performance gel-filtration involved a Varian MicroPak TSK G2000SW column (300 × 8 mm), elution with 0.1M ammonium acetate, and monitoring of the refractive index of the eluate.

For the n.m.r. experiments, S4 was depolymerised slightly by sonication of the sample in the n.m.r. tube[8].

Depyruvated polysaccharide **2**. — A solution of S4 (**1**, 75 mg) in 0.01M hydrochloric acid (10 mL) was heated at 100° for 60 min, cooled, and neutralised (0.2M ammonia). The solvent was evaporated, the residue was desalted by elution from a column (96 × 1.6 cm) of BioGel P4 with aqueous 2% ammonium hydrogen carbonate, and the eluate was lyophilised.

Tetrasaccharide **3a**. — To a solution of **2** in 0.1M ammonium acetate (pH 3.9, 5 mL) was added sodium periodate (30 mg), and the mixture was stirred at room temperature for 60 min, then overnight at 4° in the dark. Excess of periodate was reduced by the addition of ethane-1,2-diol. Polymeric material was recovered by dialysis

and treated with sodium borohydride (200 mg) for 4 h. The solution was neutralised with acetic acid, dialysed overnight, then concentrated to ~2 mL *in vacuo*, and desalted on a column of BioGel P4. The polymer was hydrolysed in 2M trifluoroacetic acid at room temperature for 16 h, and the tetrasaccharide fraction was isolated by gel-filtration on BioGel P4. The desired tetrasaccharide **3a** was isolated by h.p.l.c. on an aminopropyl column (250 × 4.6 mm, Jones Chromatography) by elution[9] with 70:30 acetonitrile–15mM sodium phosphate (pH 5.2). The eluate was monitored with a Waters 401 differential refractometer.

N.m.r. spectroscopy. — ^{1}H-N.m.r. spectra were recorded with Bruker AM500 and AM400 spectrometers under the control of Aspect 3000 computers running current DISNMR software.

^{13}C-N.m.r. spectra were obtained with a Bruker AM500, AM400, or WH270 spectrometer (under Aspect 2000 control, running FTQNMR version 820601.5). Standard Bruker microprograms were used as supplied.

Spectra of the polysaccharides were obtained at an indicated probe temperature of 70° and the oligosaccharide at 30° unless otherwise indicated. The ^{1}H-n.m.r. spectra were referenced to internal 3-(trimethylsilyl)propionic-*2,2,3,3-d*$_4$ acid at 0 p.p.m. ^{13}C-N.m.r. spectra were referenced to external 1,4-dioxane at 67.4 p.p.m. The ^{1}H correlation spectra were run at 500 MHz, using the COSY-45 pulse sequence[10], with a relaxation delay of 3 s between pulse sequences and a digital resolution of ~1.2 Hz/point in both domains, except for a double-quantum-filtered phase-sensitive COSY obtained on **2** at 20°.

The phase-sensitive NOESY spectrum of S4 (**1**) was obtained at 400 MHz and 70°, using the pulse sequence of Bodenhausen *et al.*[11]. Mixing times of 50 or 100 ms were used with random variations of ± 20 ms; 512 experiments of 32 scans were collected to give a final digital resolution of 2.0 Hz in both domains. The spectrum was processed using $\pi/2$-shifted sine-bell window functions in both domains.

1D N.O.e. experiments. — 1D Truncated-driven n.O.e. difference spectra[12] of the depyruvated polysaccharide (**2**) were obtained at 500 MHz and 70°, using a pre-irradiation time of 0.2 s and a relaxation delay of 3 s. 8K Data points were collected with inter-leaved accumulation of 32 scans up to a total of 512 transients. Amide proton resonances were observed for solutions in H_2O–D_2O (4:1) at 400 (**1**) or 500 MHz (**2** and **3a**), using the $1\bar{3}3\bar{1}$ pulse sequence[13] at various temperatures.

^{13}C,^{1}H-Correlation spectra were obtained by the method of Bax and Morris[14], for **1** at 100 MHz (^{13}C) and 65° with 4K data points in f2 and 512 increments in f1, sweep widths of 12 000 Hz in f2 and 2016 Hz in f1, and with the COLOC[15] experiment for **1** and **2** at 70° modified for observation of one-bond ^{13}C,^{1}H correlations[16]. A fixed delay, T, of 10.58 ms and 44 increments in t_1 were used, and, at each increment, 960 scans (for **1**) or 1280 scans (for **2**) of 8K data points were collected, and the spectrum was processed with a $\pi/2$-shifted (sine-bell)^2 function in f2 and a $\pi/2$-shifted sine-bell function in f1. The ^{13}C T_1 measurements were obtained at 70° and 100 MHz, using an inversion–recovery sequence[17], and the T_2 measurements were obtained at 100 MHz with a Hahn spin-echo experiment[18].

Computational methods. — Computer modelling was carried out with a ChemX system (Chemical Design Ltd., Oxford) operated with a MicroVax II (Digital Equipment). Charges were calculated using the Gasteiger algorithm[19]. Monosaccharide residues were optimised using Allinger's MM2 program[20] (Quantum Chemistry Program Exchange, Indiana University, QCPE No. 501) modified according to Jeffrey and Taylor[21] ("MM2CARB"). Oligosaccharides were built-up using initial glycosidic bond lengths of 1.40 Å and a C–O–C bond angle of 115°. Low-energy conformers, consistent with n.O.e. constraints, were found by a grid-search procedure about the two glycosidic bonds, using a simple non-bonded interaction energy, and further minimised using the MM2CARB program (see text).

The temperature dependence of time-averaged geometrical parameters was calculated as follows. Model disaccharides lacking hydroxyl protons were generated from the computer model of the depyruvated decasaccharide **4**, a grid search was performed about the glycosidic linkage at intervals of 5°, and energies were calculated using a van der Waals force field. Conformations within 5 kcal/mol of the global minimum (typically 100–350 conformations, 2–7% of conformational space) were "accepted", the energy and relevant geometrical parameters for each conformer were extracted from the computer file, and the data were passed to a commercial spreadsheet package. Relative populations of these conformers were calculated at 20° and 70° from the Boltzman equation and time-averaged dihedral angles, distances, *etc.* at the two temperatures were determined.

N.O.e. simulations used the program NOEMOL[22] running on a SUN3/160, using an isotropic tumbling model with a single effective correlation time of 10 ns derived by fitting the α-Gal H-1 to H-2 intra-residue n.O.e.

RESULTS

Preparation of samples. — Depyruvation, and probably slight depolymerisation, of S4 (**1**) in dilute acid resulted in a sample that gave ^{1}H lines narrower than those of S4. Depyruvation was complete as judged by ^{1}H-n.m.r. spectroscopy. Depyruvated S4 (**2**) was subjected to Smith degradation[5] and yielded a mixture of tetrasaccharide derivatives that were isolated by gel-filtration and fractionated by h.p.l.c. to give the pure tetrasaccharide derivative **3a**.

^{1}H-N.m.r. assignments. — S4 (**1**) gave a poorly resolved spectrum (Fig. 1) due to fast proton T_2 relaxation, even after sonication and at 70°, so that a full assignment could not be made from the COSY-45 spectrum alone, but was completed with data from 1D n.O.e. difference and phase-sensitive NOESY experiments. Depyruvated S4 (**2**) at 70° gave well resolved spectra, an almost complete assignment of the spin systems could be made from the COSY-45 spectrum, and most of the polymer n.m.r. studies were carried out on this sample (Fig. 2). The COSY-45 spectrum had sufficient digital resolution (1.2 Hz/point) so that the fine structure of the correlation peaks yielded approximate coupling constants. The spin system arising from the β-ManNAc residue was assigned on the basis of the J values ($J_{1,2}$ small, $J_{3,4} \sim 10$ Hz). The α-Gal spin system

was assigned on the basis of the large shift of the H-1 resonance on depyruvation and the high-field position of the H-2 resonance (compared to its position in the HexNAc). A cross-peak in the NOESY spectrum between the single H-4 resonance at 4.009 p.p.m. and the signal (q) at 4.097 p.p.m. which, in turn, correlated with the methyl group at 1.250 p.p.m., established this as part of the FucNAc spin system. A 1D n.O.e. difference experiment with pre-irradiation of the FucNAc methyl group resulted in strong enhancements of the H-5 and H-4 resonances at 4.097 and 4.009 p.p.m., respectively, confirming these assignments which accord with data on the tetrasaccharide derivative **3a** and the observed inter-residue n.O.e.'s.

The remaining ambiguity in the spectrum of the depyruvated polysaccharide **2** was resolved by the use of a 1D n.O.e. difference experiment[2b]. The Gal H-4 and GalNAc H-4 resonances were coincident at 4.05 p.p.m. and the H-4/H-5 cross peaks could not be observed due to the small $J_{4,5}$ value (typically 0.8 Hz). The two H-5/H-6a/H-6b spin systems were observed in the COSY spectrum, with the H-5 resonances (2 t) at 4.140 and 4.404 p.p.m. An n.O.e. difference spectrum with pre-irradiation of [α-Gal H-3 + β-ManNAc H-6a] resulted in enhancement of the H-5 resonance at 4.14 p.p.m. (t, 6 Hz), which, therefore, was assigned to the α-Gal residue. The α-Gal H-3–H-5 distance was determined to be 2.52 Å in computer models[23]. The assignment of the α-GalNAc H-5 resonance was made by default, but was consistent with all subsequent experiments. The downfield shift of the α-GalNAc H-5 resonance is consistent with its close proximity to the α-Gal O-3 (see below). The assignment of the spectrum (Fig. 1) of the tetrasaccharide derivative **3a** from the COSY-45 experiment was straightforward. These assignments are summarised in Table I. For **1**, **2**, and **3a**, the chemical shifts of the α-FucNAc H-2 and H-3 resonances (4.200 and 4.166 p.p.m., respectively, in **2**) are considerably different from those of α-GalNAc H-2 and H-3 (4.427 and 3.959 p.p.m., respectively), although these residues are in similar environments. The conformational analysis must be able to account for such differences.

Chemical shifts for the resonances in depyruvated S4 (**2**) were also determined from a double-quantum-filtered phase-sensitive COSY at 20° for analysis of the temperature-dependent, time-averaged, inter-residue proton–oxygen distances.

The 1D ^{1}H-n.m.r. spectra of S4 (**1**) and depyruvated S4 (**2**) each contained a strong resonance at 3.24 p.p.m., typical of the trimethylammonium group of a choline phosphate substituent, and the COSY-45 spectra showed minor cross-peaks indicative of 3.5% pneumococcal C-substance in this sample[24].

Inter-proton coupling constants. — Values for $^3J_{H,H}$ were measured from the 1D spectra where possible or could be estimated from the fine structure of cross-peaks in the COSY-45 spectrum. Additionally, a *J*-resolved spectrum was obtained for the tetrasaccharide derivative **3a**. The $^3J_{H,H}$ values accorded with the expected $^4C_1$ conformation for the D sugars and $^1C_4$ conformation for the L-FucNAc, and with the assignments in Table I.

Conformation of the hydroxymethyl groups. — The H-5,6a,6b coupling constants and chemical shifts give information on the time-averaged conformations of the hydroxymethyl groups, which appeared to be the same in **2** and **3a**. The $J_{5,6a}$ and $J_{5,6b}$ values

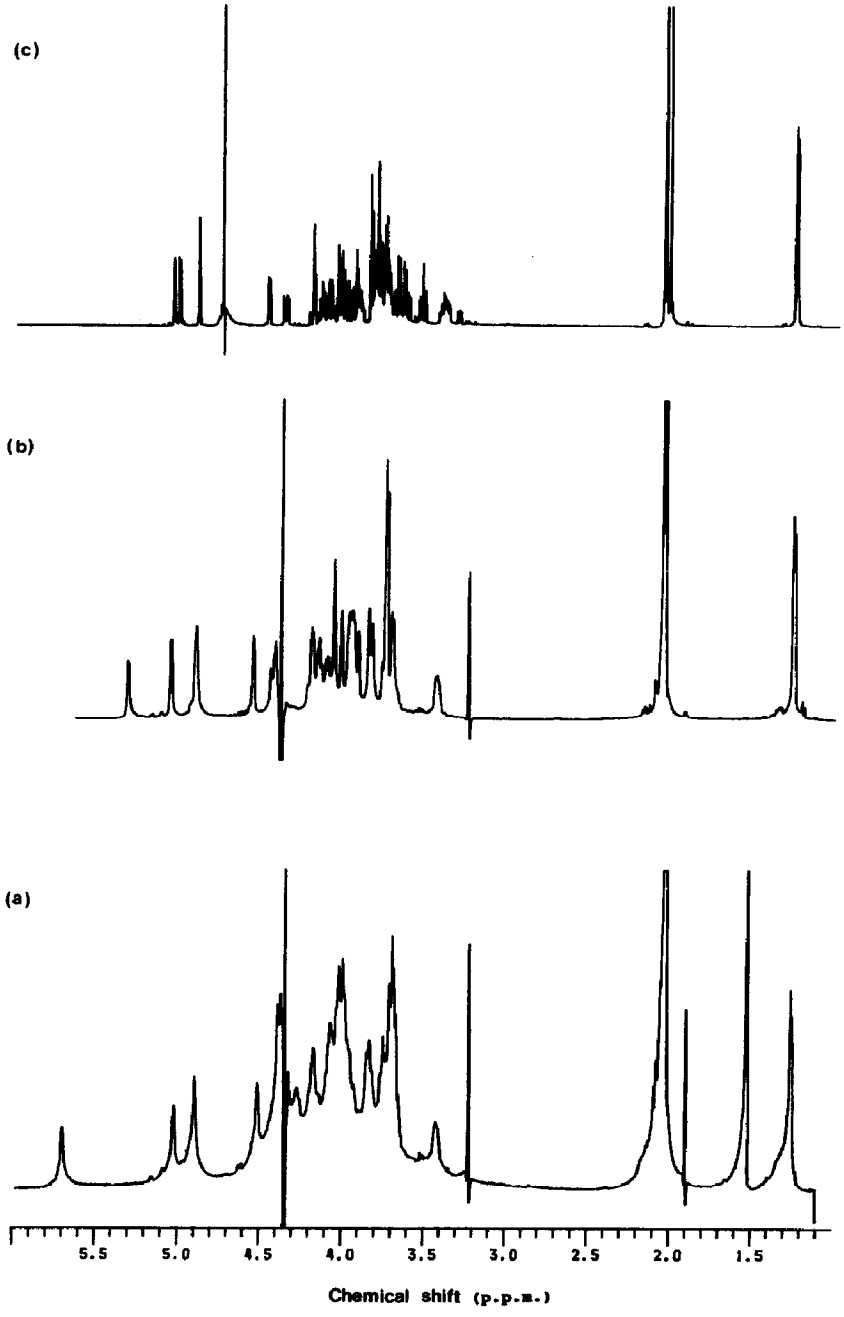

Fig. 1. 1D ^{1}H-N.m.r. of (a) S4 (**1**, 500 MHz, 70°), (b) depyruvated S4 (**2**, 500 MHz, 70°), and (c) the tetrasaccharide derivative **3a** (500 MHz, 30°).

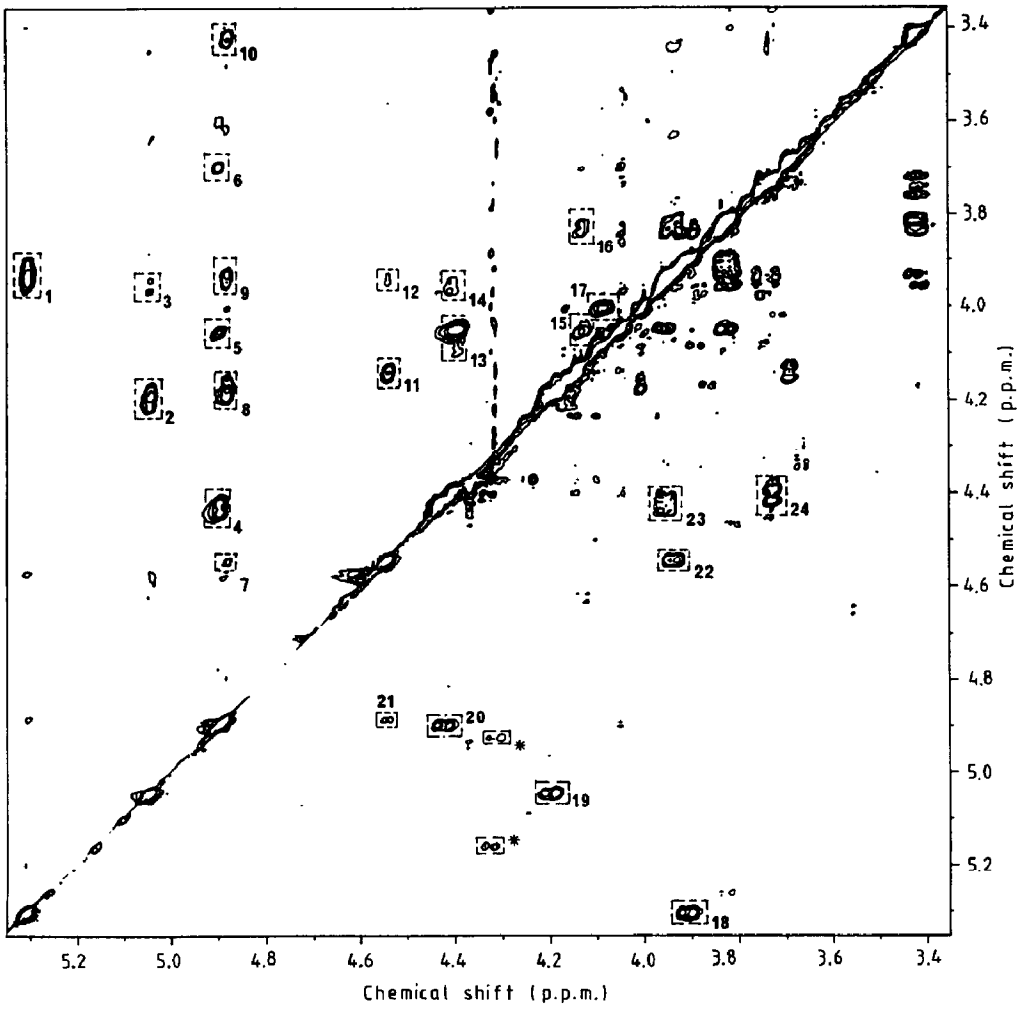

Fig. 2. The phase-sensitive NOESY spectrum (400 MHz) and COSY-45 spectrum (500 MHz) of depyruvated S4 (2) at 70°. The numbered cross-peaks are assigned as follows: (1) α-Gal H-1/α-Gal H-2 and β-ManNAc H-3, (2) α-FucNAc H-1/α-FucNAc H-2, (3) α-FucNAc H-1/α-GalNAc H-3, (4) α-GalNAc H-1/α-GalNAc H-2, (5) α-GalNAc H-1/α-Gal H-4, (6) α-GalNAc H-1/α-Gal H-6,6, (7) β-ManNac H-1/β-ManNAc H-2, (8) β-ManNAc H-1/α-FucNAc H-3, (9) β-ManNAc H-1/β-ManNAc H-3, (10) β-ManNAc H-1/β-ManNAc H-5, (11) β-ManNAc H-2/α-Gal H-5, (12) β-ManNAc H-2/β-ManNAc H-3, (13) α-GalNAc H-5/α-GalNAc H-4, (14) α-GalNAc H-5/α-GalNAc H-3, (15) α-Gal H-5/α-Gal H-4, (16) α-Gal H-5/α-Gal H-3, (17) α-FucNAc H-4/α-FucNAc H-5, (18) α-Gal H-1/α-Gal H-2, (19) α-FucNAc H-1/α-FucNAc H-2, (20) α-GalNAc H-1/α-GalNAc H-2, (21) α-ManNAc H-1/β-ManNAc H-2, (22) α-ManNAc H-2/β-ManNAc H-3, (23) α-GalNAc H-2/α-GalNAc H-3, (24) α-GalNAc H-5/α-GalNAc H-6,6.

(6 Hz) and the similar chemical shifts for the H-6a,6b resonances in the Gal and GalNAc residues are consistent with a conformational equilibrium between three rotamers, with *gt* preponderant. The $J_{5,6a}$ and $J_{5,6b}$ values of 2 and 5 Hz, respectively, and the observed chemical shifts, are consistent with the usual equilibrium[25] between *gg* and *gt* rotamers for the ManNAc residue.

TABLE I

^{1}H-N.m.r. assignments of S4 (**1**), depyruvated S4 (**2**), and the tetrasaccharide derivative (**3a**)

Residue	*H-1*	*H-2*	*H-3*	*H-4*	*H-5*	*H-6*	*H-6'*	*NAc*
β-ManNAc **1**[a]	4.893	4.503	4.019	3.750	3.415	3.938	3.823	(2.018)[d]
β-ManNAc **2**[a]	4.886	4.546	3.943	3.746	3.423	3.949	3.827	(2.035)
β-ManNAc **2**[b]	4.910	4.539	3.965	3.736	3.412	3.922	3.822	(2.032)
β-ManNAc **3a**[c]	4.894	4.465	3.817	3.533	3.383	3.938	3.824	(2.020)
α-FucNAc **1**[a]	5.018	4.179	4.160	3.990	4.078	1.251		(2.029)
α-FucNAc **2**[a]	5.044	4.200	4.166	4.009	4.097	1.250		(2.045)
α-FucNAc **2**[b]	5.045	4.178	4.189	4.043	4.102	1.250		(2.042)
α-FucNAc **3a**[c]	5.044	4.205	4.166	4.012	4.093	1.251		(2.050)
α-GalNAc **1**[a]	4.892	4.376	3.940	3.997	4.287	3.692	3.692	(2.029)
α-GalNAc **2**[a]	4.896	4.427	3.959	4.052	4.404	3.736	3.736	(2.045)
α-GalNAc **2**[b]	4.877	4.418	3.987	4.059	4.461	3.713	3.713	(2.053)
α-GalNAc **3a**[c]	5.008	4.363	3.978	4.048	4.141	3.76	3.76	(2.050)
α-Gal **1**[a]	5.693	4.016	3.959	4.376	4.058	3.695	3.695	1.522
α-Gal **2**[a]	5.303	3.914	3.831	4.054	4.140	3.697	3.697	
α-Gal **2**[b]	5.302	3.914	3.822	4.034	4.168	3.693		
Threitol **3a**[c]		3.627	3.686	3.913	3.732	3.80	3.80	

[a] Data obtained at 70°. [b] Data obtained at 20°. [c] Data obtained at 30°. [d] Tentative assignments in brackets.

Amide proton resonances. — The NH resonances of **1**, **2**, and **3a** were observed when spectra were obtained for solutions in H_2O–D_2O (4:1), using the $1\bar{3}3\bar{1}$ pulse sequence for water suppression[13]. Careful desalting was necessary in order to suppress fast chemical exchange at the higher temperatures. The *J* values measured for the tetrasaccharide derivative **3a** are consistent with a preponderantly *trans* arrangement of NH and H-2 in the time-averaged conformations when compared to the Karplus curve for H–C–N(CO)–H in peptides[26], and are consistent with the observed conformation of *N*-acetyl groups in glycopeptides[27]. The resonance at 7.583 p.p.m. was assigned tentatively to NH of the ManNAc residue due to its large coupling (> 10 Hz), as found in monosaccharide model systems. Accurate coupling constants were more difficult to obtain for the polymers, but they were consistent with a *trans* arrangement. The temperature dependence of the chemical shift of the amide protons was very similar in each of the three samples, and to those of monosaccharide model systems, suggesting that the amide protons are not involved in intramolecular hydrogen bonding. For **1**, the peak at 7.524 p.p.m. (at 70°) showed considerable broadening at higher temperatures, suggestive of an increased rate of exchange compared to the other amide protons. These data are summarised in Fig. 3.

^{13}C-N.m.r. spectra. — (*a*) *Assignments.* The carbon spectra of S4 (**1**) and derivatives **2** and **3a** are shown in Fig. 4. Assignments of the ^{13}C resonances of S4 (**1**) was attempted by ^{13}C-detected ^{13}C,^{1}H correlation at 100 MHz, using the method of Bax and

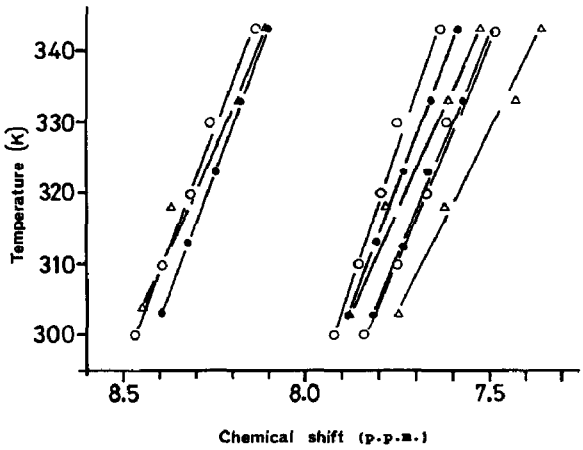

Fig. 3. Temperature-dependence of the chemical shifts of the amide proton resonances. Spectra were measured using the 1331 pulse sequence and chemical shifts (internal trimethylsilylpropionic acid at 0 p.p.m.) plotted against the indicated probe temperature. Spectra were obtained at 400 or 500 MHz: △, S4 (**1**); ○, depyruvated S4 (**2**); ●, tetrasaccharide derivative (**3a**).

Morris[14], and the assignments of Jansson *et al.*[2a]. Only a subset of the expected cross-peaks could be observed (primarily those from the α-GalNAc residue) due to differences in the rates of relaxation between the individual sugar residues, and a COLOC experiment[15] tuned for one-bond $^{13}C,^{1}H$ coupling constants[16] was used. This method was of value in studies of viscous polysaccharides[16b], but delivers poor digital resolution in the ^{1}H domain. This spectrum showed an almost complete set of $^{13}C,^{1}H$ correlation peaks, although cross-peaks from two of the anomeric positions were missing. Where resonances overlapped in the ^{1}H-n.m.r. spectrum, ambiguities were resolved using chemical shift arguments[28], except for the Gal and GalNAc C-6 resonances and the α-Gal C-2,3,5 resonances, where both the ^{1}H and ^{13}C resonances were overlapped. The α-Gal and α-GalNAc C-6 resonances were distinguished on the basis of the effects of temperature on the chemical shift in the pyruvated and depyruvated system and the relaxation data (see below). These assignments are given in Table II. The ^{13}C-n.m.r. spectrum of the depyruvated S4 (**2**) was obtained also from a COLOC experiment, and, as both the ^{13}C- and ^{1}H-n.m.r. spectra are well resolved, a full assignment was made. This spectrum is shown in Fig. 5. Tentative assignments for the tetrasaccharide **3a** are from Jansson *et al.*[2a], chemical shift arguments, and comparison with the polysaccharide samples.

(*b*) *Variable temperature studies.* The ^{13}C-n.m.r. spectra of S4 (**1**), depyruvated S4 (**2**), and the tetrasaccharide derivative (**3a**) were obtained at a range of temperatures (27–77°), and the results for the resolved peaks (Fig. 6) showed quite marked temperature dependence for several resonances. The patterns of movement were similar in the three samples, apart from the signals from one hydroxymethyl group and the α-GalNAc C-5 resonance which had temperature coefficients of opposite sign in **1** from those in **2** and **3a**. These data were interpreted as showing similar conformational variation with

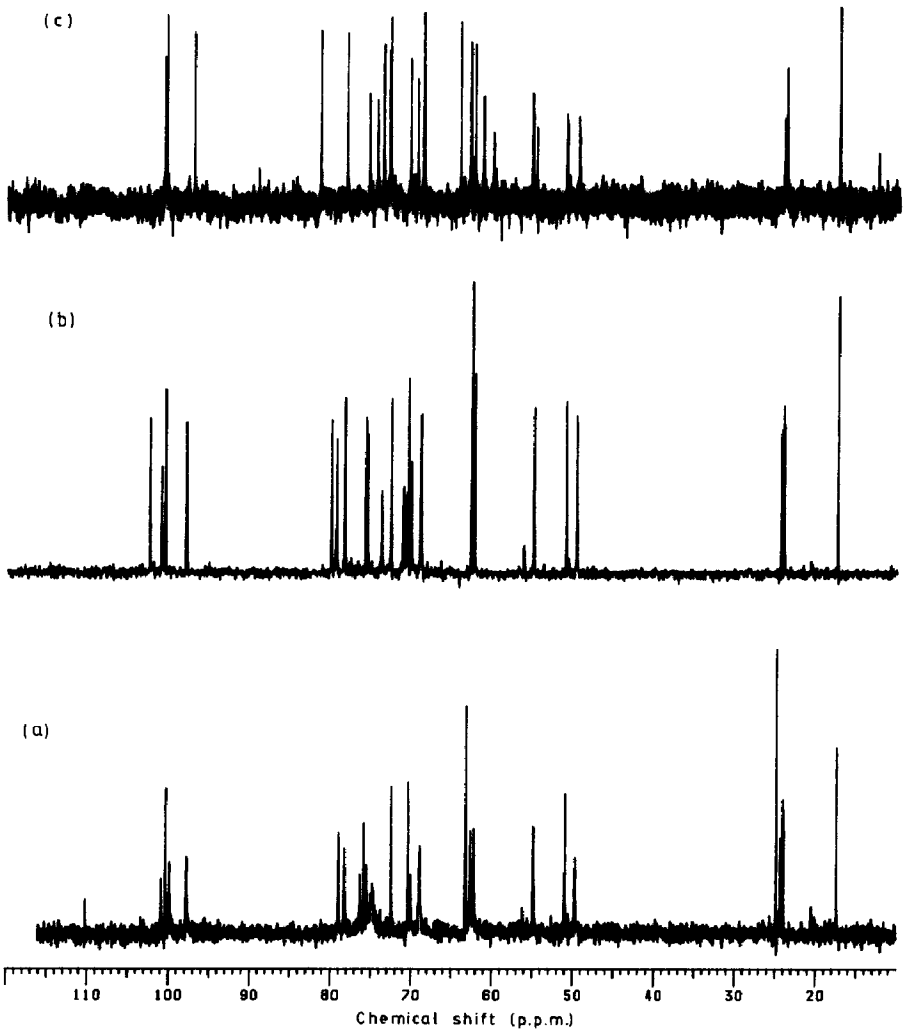

Fig. 4. 1D ^{1}H-Decoupled ^{13}C-n.m.r. spectra of (a) S4 (**1**), (b) depyruvated S4 (**2**), and (c) the tetrasaccharide derivative **3a**; (a) and (b) at 100 MHz and 70°, and (c) at 125 MHz and 35°.

temperature, and, by implication, similar overall conformations for **1**, **2**, and **3a**. The similarity between the data (Table III) for the polysaccharides **1** and **2** and the tetrasaccharide **3a** (where incomplete assignments are available) excludes an important contribution to the conformation from such "macromolecular" effects as gelling or the formation of internally stabilised (hydrogen-bonded) helices, although these have been postulated for the meningococcal type b polysaccharide[29]. The largest temperature coefficients are associated with the glycosylated C-3s.

(*c*) *Carbon relaxation studies.* The spin–lattice relaxation rates ($R_1 = 1/T_1$) of the methine carbons in **1** and **2**, determined by the inversion–recovery method[17], were constant within error limits (Table IV), and were similar for the methine and methylene

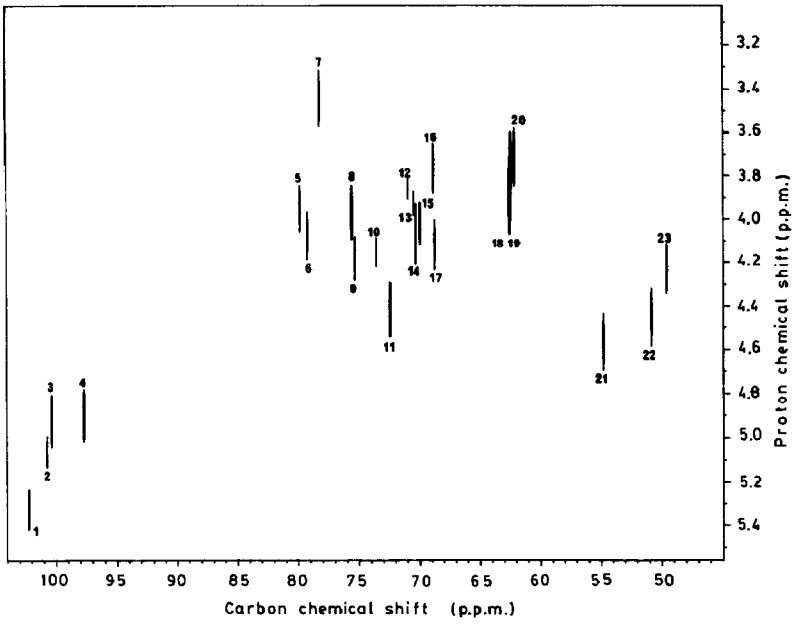

Fig. 5. Partial COLOC spectrum tuned for $^{1}J_{C,H}$ of the depyruvated S4 (**2**), obtained at 100 MHz and 70°, showing the methine carbons. Peak labelling is as follows: (1) Gal C-1, (2) FucNAc C-1, (3) GalNAc C-1, (4) ManNAc C-1, (5) ManNAc C-3, (6) Gal C-4, (7) ManNAc C-5, (8) GalNAc C-3, (9) FucNAc C-3, (10) Gal C-5, (11) GalNAc C-5, (12) Gal C-3, (13) Gal C-2, (14) GalNAc C-4, (15) FucNAc C-4, (16) ManNAc C-4, (17) FucNAc C-5, (18) and (19) ManNAc C-6 and GalNAc C-6, (20) Gal C-6, (21) ManNAc C-2, (22) GalNAc C-2, (23) FucNAc C-2.

TABLE II

^{13}C Chemical shift assignments

Residue	*C-1*	*C-2*	*C-3*	*C-4*	*C-5*	*C-6*
β-ManNAc **1**	97.7[a]	54.7[a,c]	78.9[a]	68.9[a]	78.1[a]	62.6[a,c]
β-ManNAc **2**	97.8[a,c]	54.9[a,c]	79.8[a]	68.9[a]	78.2[a]	62.2[a]
β-ManNAc **3a**	97.7[c]	55.2[c]			78.2[b]	
α-FucNAc **1**	100.7[c]	49.6[c]	75.4[a]	69.9[a,f]	68.8[a]	17.3[a]
α-FucNAc **2**	100.9[a,c]	49.5[a,c]	75.4[a]	70.0[a]	68.8	17.3[c]
α-FucNAc **3a**	100.9[c]	49.5[c]		69.5[b]	68.8[b]	17.3[c]
α-GalNAc **1**	100.2[a]	50.8[a]	75.7[a]	70.3[a,f]	72.3[a]	63.1[a,d]
α-GalNAc **2**	100.3[a,c]	50.9[a,c]	75.6[a]	70.4[a]	72.4[a]	62.5[a]
α-GalNAc **3a**	100.5[c]	50.9[c]	75.5[b]	70.4[b]	72.8[b]	
α-Gal **1**	99.7[b]	74.8[e]	74.6[e]	76.2[a]	75.6[e]	62.1[a,d]
α-Gal **2**	102.3[c]	70.5[a]	70.9[a]	79.2[a]	73.6[a]	62.2[a]
Threitol **3a**				81.5[b]		
Pyruvic acetal		110.0[b]	24.7[a]			

[a] Cross-peak observed in X–H correlation experiment. [b] From the 1D ^{13}C-n.m.r. spectrum and the arguments on chemical shifts. [c] Assignments from Jansson *et al.*[2a]. [d,e,f] Assignments may be interchanged.

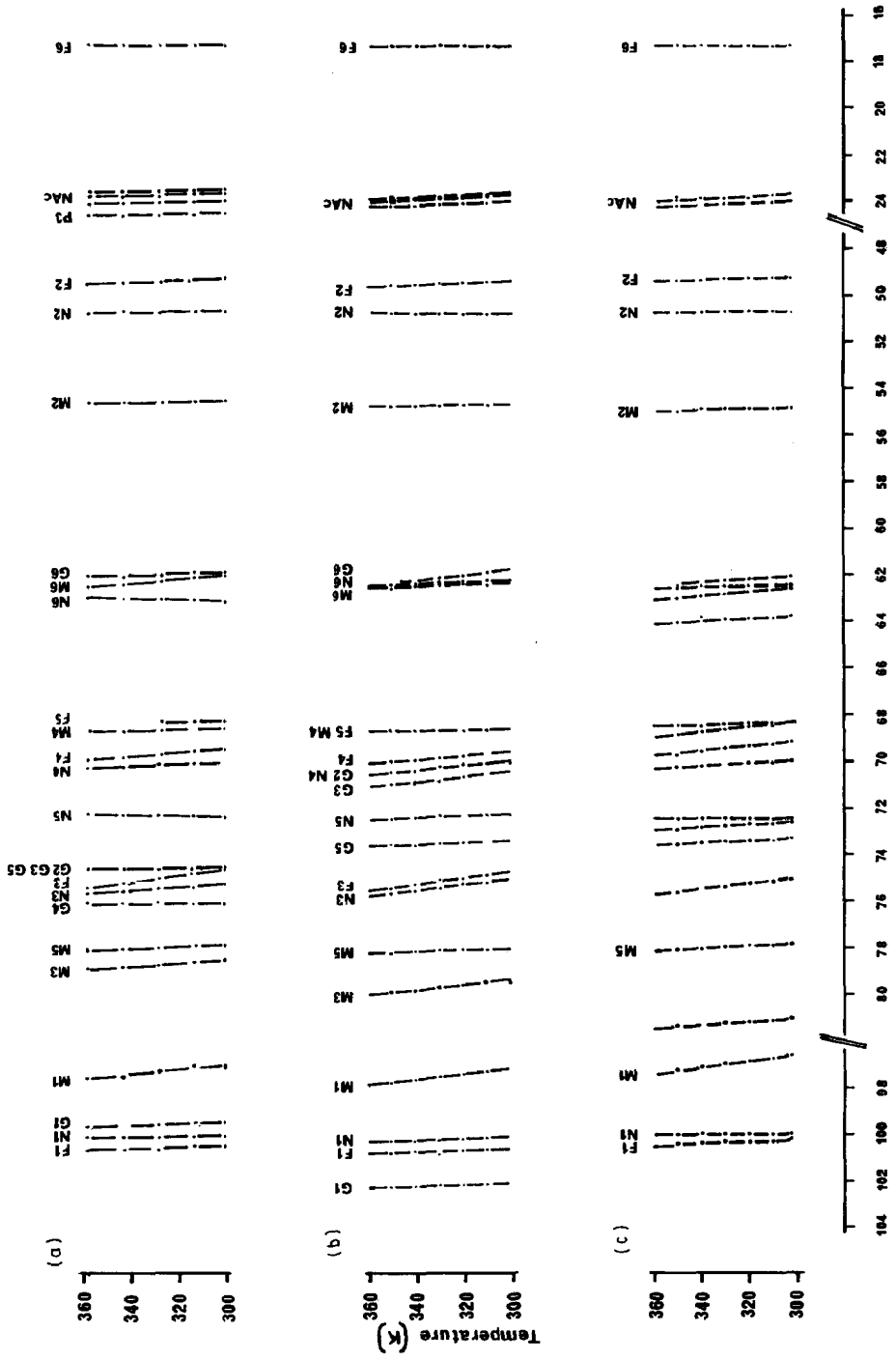

Fig. 6. Temperature dependence of the chemical shifts of the ^{13}C resonances of (a) S4 (1), (b) depyruvated S4 (2), and (c) the tetrasaccharide derivative 3a. The spectra were obtained at 67.95 MHz and referenced internally against the FucNAc C-6 signal at 17.3 p.p.m.

TABLE III

Temperature coefficients[a] of ^{13}C chemical shifts for **1**, **2**, and **3a**

Residue	*C-1*	*C-2*	*C-3*	*C-4*	*C-5*	*C-6*
ManNAc (**1**)	11.0	2.2	6.2	2.2	4.8	9.1
ManNAc (**2**)	13.2	1.7	11.5	6.0	4.8	4.2
ManNAc (**3a**)	12.8	2.4			4.8	8.3
FucNAc (**1**)	3.8	4.1	14.1	8.4	10.0	zero
FucNAc (**2**)	5.8	4.2	14.3	8.0	2	zero
FucNAc (**3a**)	4.6	3.4				zero
GalNAc (**1**)	1.7	1.0	8.4	3.6	−1.3	−2.7
GalNAc (**2**)	4.2	1.2	11.0	10.5	4.3	6.0
GalNAc (**3a**)	0.2	0.4				2.2
Gal (**1**)	4.1	(———11.2———)		0.0	(11.2)	2.9
Gal (**2**)	3.0	11.7	5.5	5.3	5.0	14.2

[a] In p.p.b.; a downfield shift with increasing temperature is positive.

carbons in the two samples, except for the resonance assigned to α-GalNAc C-6. Carbon spin–spin relaxation rates (R_2) were obtained from Hahn spin-echo experiments[18] using composite pulse proton decoupling. In S4 (**1**), the different residues had different relaxation rates, with fast relaxation for the pyruvated α-Gal residue, although the C-2,3,5 resonances formed an overlapping envelope. For depyruvated S4 (**2**), the relaxation rates are lower and show less variation between residues. Although interpretation of these rates is difficult, the general trend is clear, and in qualitative agreement with other n.m.r. data and the difference in viscosity between the two samples.

A recent study[30] of the relaxation behaviour of C-1 in ^{13}C-labelled hepatic glycogen concluded that spin–lattice relaxation rates are dominated by local motion, whereas spin–spin relaxation rates are determined primarily by T_M, the correlation time for overall motion.

Inter-proton n.O.e. experiments. — 1D Truncated-driven n.O.e. experiments[12] were carried out on the tetrasaccharide derivative **3a**, depyruvated S4 (**2**), and S4 (**1**), and phase sensitive NOESY spectra were obtained for **2** and **1**. The tetrasaccharide derivative gave small positive n.O.e.'s (400 MHz, 30°), whereas the polymers gave large negative n.O.e.'s (500 MHz, 70°). Initial experiments with depyruvated S4, using pre-irradiation times between 0.05 and 2 s, showed that, at 0.2 s, clean, intense n.O.e. difference spectra with little spin diffusion were obtained. This pre-irradiation time was used for subsequent experiments. The rate of build-up of intra-residue n.O.e.'s was used to estimate an effective correlation time for n.O.e. simulation calculations (see below).

With a short pre-irradiation time, the rate of n.O.e. build-up is approximately linear, and the magnitude of the n.O.e. is proportional to the cross-relaxation rate (σ). Several inter-residue n.O.e.'s confirmed the sequence, but required a revision of the

TABLE IV

^{13}C Relaxation rate data (s^{-1}) for S4 (**1**) and depyruvated S4 (**2**) at 70° and 100 MHz

Residue	*C-1*	*C-2*	*C-3*	*C-4*	*C-5*	*C-6*
ManNAc (**1**)	2.94 ±0.16	3.12 ±0.11	2.60 ±0.15	2.61 ±0.15	2.64 ±0.16	4.52 ±0.19
ManNAc (**2**)	3.15 ±0.12	3.10 ±0.06	3.09 ±0.11	2.98 ±0.13	2.98 ±0.08	4.93 ±0.16
FucNAc (**1**)	3.14 ±0.24	2.93 ±0.28	2.91 ±0.14	2.73 ±0.18	2.61 ±0.16	1.17 ±0.07
FucNAc (**2**)	3.26 ±0.29	2.90 ±0.07	2.78 ±0.06	2.93 ±0.13	2.89 ±0.08	1.22 ±0.03
GalNAc (**1**)	3.16 ±0.13	3.15 ±0.14	3.06 ±0.04	3.25 ±0.06	3.46 ±0.11	3.49 ±0.06
GalNAc (**2**)	3.17 ±0.12	3.29 ±0.12	3.30 ±0.15	3.07 ±0.04	3.24 ±0.16	2.66 ±0.07
Gal (**1**)	2.96 ±0.14	(2.69 ±0.35	2.92 ±0.16)	2.99 ±0.12	(3.01 ±0.20)	3.68 ±0.18
Gal (**2**)	2.98 ±0.08	3.03 ±0.22	3.17 ±0.15	2.92 ±0.10	3.30 ±0.13	3.68 ±0.11
Carbon spin–spin relaxation rates (s^{-1})						
ManNAc (**1**)	25.97 ±1.27	18.20 ±1.04	20.87 ±1.28	29.11 ±1.34	20.84 ±1.77	22.20 ±1.26
ManNAc (**2**)	9.60 ±0.25	8.92 ±0.30	10.42 ±0.17	9.57 ±0.41	7.60 ±0.38	9.45 ±0.13
FucNAc (**1**)	28.08 ±1.90	23.07 ±2.16	38.06 ±1.53	35.93 ±2.37	24.83 ±1.86	
FucNAc (**2**)	11.86 ±0.66	8.83 ±0.32	9.48 ±0.88	11.11 ±1.83	10.66 ±0.50	
GalNAc (**1**)	11.41 ±0.27	14.65 ±0.30	22.62 ±2.16	9.81 ±0.45	12.68 ±0.55	9.27 ±0.27
GalNAc (**2**)	6.23 ±0.19	8.82 ±0.28	8.81 ±0.26	6.26 ±0.15	7.05 ±0.11	5.12 ±0.14
Gal (**1**)	29.17 ±2.69	(——43.50 ±7.5——)		32.50 ±2.07	(43.5 ±7.5)	27.40 ±1.37
Gal (**2**)	8.73 ±0.29	21.28 ±1.28	21.58 ±0.83	10.98 ±0.67	17.92 ±0.33	9.25 ±0.39

reported linkage between the Gal and ManNAc residues[2b]. These inter-residue n.O.e.'s were quantified and several constraints for the molecular modelling were obtained (see below). That these constraints are estimates must be emphasised; the resolution enhancement needed to resolve adjacent peaks, unresolved peaks, the presence of spin diffusion, and problems associated with ensuring a flat baseline all degrade the quality of the results. Control experiments in which well-resolved peaks in n.O.e. difference spectra, processed with or without enhancement by Lorentzian to Gaussian transformation, suggested that the resolution enhancement did not introduce significant errors.

N.O.e. difference experiments on S4 (**1**) were performed using a pre-irradiation time of 0.1 s which allowed the assignment of some resonances not assigned by the correlation methods and the determination of the stereochemistry at the C-2 of the pyruvic acetal. The observed intra- and inter-residue n.O.e.'s for the polysaccharides **1** and **2** are shown in Table V. At 70°, the α-GalNAc H-2 and H-5 resonances are obscured by the residual water signal, and n.O.e.'s of these resonances could not be quantified. The strongest inter-residue n.O.e. arising from pre-irradiation of H-1 was at the proton at the other end of the glycosidic bond, *e.g.*, α-Gal H-1 to β-ManNAc H-3, and this was typically 20–30% except that the n.O.e. of the α-GalNAc H-3 due to irradiation of the α-FucNAc H-1 was only 13%.

The phase-sensitive NOESY experiments were carried out in order to complete the spectral assignments and provide a complete map of inter-residues n.O.e.'s for modelling, rather than quantitative information. Using a mixing time of 0.1 s, the

TABLE V

Experimental and simulated n.O.e.'s in the depyruvated S4 (2) and the model (4)

Proton irradiated		*Exptl. data (2)*	*MM2 Energy minimised (4)*	*N.m.r. finessed*
α-Gal H-1	α-Gal H-2	33	32.6	33.2
	α-Gal H-3 + β-ManNAc H-6a	9	6.2	6.0
	β-ManNAc H-1 + α-GalNAc H-1	14	5.2	6.6
	β-ManNAc H-2	8	6.4	8.7
	β-ManNAc H-3 + α-GalNAc H-3 + β-ManNAc H-6b	34	24.6	33.4
	β-ManNAc H-4	14	5.1	9.3
	β-ManNAc H-5	11	4.2	5.4
	α-FucNAc H-1	3	0.5	0.3
α-FucNAc H-1	α-FucNAc H-2/H-3	49	41.7	40.9
	α-FucNAc H-4	4	2.6	2.6
	α-Gal H-1	2	0.6	0.3
	α-GalNAc H-3	13	39.6	12.8
	α-GalNAc H-4	3	10.2	4.8
	β-ManNAc H-1 + α-GalNAc H-1	8	3.0	2.8
	β-ManNAc H-2	2	0.5	0.5
	β-ManNAc H-5	4	0.5	0.6
β-ManNAc H-1 + α-GalNAc H-1	β-ManNAc H-2	11	29.2	30.4
	β-ManNAc H-3 + β-ManNAc H-6b + α-GalNAc H-3	45	37.5	35.0
	β-ManNAc H-5	38	35.1	34.7
	α-Gal H-1	19	6.8	8.5
	α-Gal H-3 + β-ManNAc H-6a	14	11.6	15.7
	α-GalNAc H-4 + α-Gal H-4	31	49.5	33.2
	α-Gal H-6s	35	35	35
	α-FucNAc H-1	11	3.3	3.7
	α-FucNAc H-2/H-3	59	36.2	63.9
	α-FucNAc H-4	9	24.3	14.6
β-ManNAc H-2	β-ManNAc H-1	7	23.1	24.5
	β-ManNAc H-3 + α-GalNAc H-3 + β-ManNAc H-6b	13	37.5	31.4
	α-Gal H-3 + β-ManNac H-6a	6	9.9	7.2
	α-Gal H-4	6	7.1	5.7
	α-Gal H-5	21	31.4	20.7

Proton irradiated		*Exptl. data (2)*	*MM2 Energy minimised (4)*	*N.m.r. finessed*
α-FucNAc H-2 +	α-FucNAc H-1	33	31.4	35
α-FucNAc H-3	α-FucNAc H-4	8	30.8	31.2
	β-ManNAc H-1 + α-GalNAc H-1	20	27.9	9.4
	β-ManNAc H-2	8	6.7	10.0
α-Gal H-3 +	α-Gal H-1	6	6.5	6.5
β-ManNAc H-6a	α-Gal H-2	48	10.2	18.2
	α-Gal H-4	19	26.5	28.3
	α-Gal H-5	22	19.8	20.7
	β-ManNAc H-5	11	27.1	24.5
	α-FucNAc H-1	3	0.8	1.3
	α-FucNAc H-2/H-3	6	5.5	6.0
β-ManNAc H-5	β-ManNAc H-1	15	27.9	27.9
	β-ManNAc H-2	4	9.3	9.7
	β-ManNAc H-4	15	12.8	11.6
	α-Gal H-1	7	4.8	6.0
	α-FucNAc H-1	3	0.5	0.7
	α-FucNAc H-2/H-3	15	10.9	15.0

phase-sensitive NOESY of S4 (**1**) at 400 MHz and 70° showed extensive spin diffusion, but with a mixing time of 50 ms, a "clean" spectrum was produced.

The similar patterns of inter-residue n.O.e.'s for **1** and **2** suggest that the conformations about the glycosidic bonds were similar.

Stereochemistry of the pyruvic acetal group[2c]. — For S4 (**1**), the α-Gal H-2 and H-3 resonances were assigned to peaks at 4.016 and 3.969 p.p.m., respectively, and the β-ManNAc H-3 signal to a peak at 4.013 p.p.m. overlapping that of the α-Gal H-2. An n.O.e. difference spectrum with pre-irradiation of the α-Gal H-1 showed a strong enhancement of the [α-Gal H-2 + β-ManNAc H-3] signal (the expected intra- and inter-residue N.O.e.'s), whereas pre-irradiation of the pyruvic methyl group at 1.52 p.p.m. caused an enhancement of the α-Gal H-3 resonance. These results are consistent with the pyruvic methyl group lying below the plane of the sugar ring (Fig. 7), *i.e.*, *S* stereochemistry at the pyruvic acetal C-2. This pattern of n.O.e.'s was confirmed in the phase-sensitive NOESY spectrum of S4 (**1**).

Computer modelling. — As the most comprehensive n.m.r. data are available on depyruvated S4 (**2**) at 70°, the molecular modelling was concentrated on this system, and conformational differences due to pyruvation or temperature were inferred from differences in the experimental data. The absence of charged groups on **2** was also an advantage. The inter-proton coupling constants, bond angles, and bond lengths, as noted above, were used as constraints to generate a computer model of the depyruvated decasaccharide (**4**),

ManNAc-FucNAc-GalNAc-[Gal-ManNAc-FucNAc-GalNAc-]-Gal-ManNAc-FucNAc-OMe,

A B C D E F G H I J

4

in which the central tetrasaccharide moiety represents the conformation of the repeating unit in depyruvated S4. S4 was modelled by replacement of the Gal residue with a pyruvated Gal residue, to produce **5**.

The conformational model was generated by a two-step process. Initially, a model was created using, primarily, energy minimisation to define the glycosidic angles (Fig. 8). N.O.e. constraints were added, but only to select the energy minima to be considered further when multiple minima were present. This model was then used predictively for full n.O.e. simulation and short inter-residue proton–oxygen distances, which could be distinguished experimentally by the downfield shift on the proton resonance[31]. Other simulations are possible, such as the effect of the carbonyl shielding cone. The minimum-energy model of depyruvated S4 was then adjusted to improve the fit to these experimental data.

No allowance was made in the computational force fields for the exo-anomeric effect[6], hydrogen bonding, or solvation, since the final adjustments of the model to fit the experimental data would effectively handle these aspects. Although a single, rigid, lowest-energy conformation was modelled, since there are insufficient n.m.r. data to define multiple conformations about the glycosidic bonds, the effect of mobility with a conformational space was simulated later when the variable temperature data were investigated.

Energy minimisation. Disaccharide units were constructed from MM2CARB-minimised monosaccharides, with the C-1–O-x–C-x bond set to 115°, *N*-acetyl groups (H-2–C-2–NH) *trans* and *s*-cis[32], C-1–O-x set at 1.40 Å, and O-x–C-x set at 1.410 Å. The

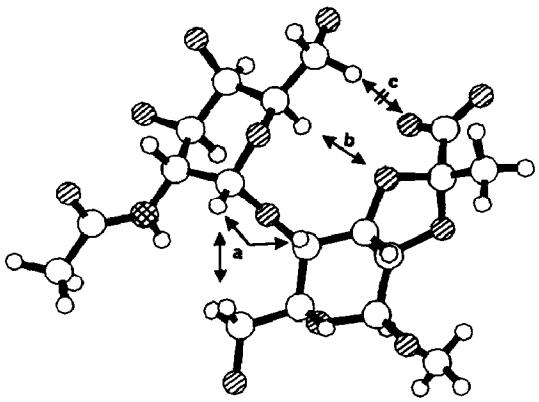

Fig. 7. The α-GalNAc-(1→4)-α-Gal(2,3-Pyr) linkage, set in the time-averaged conformation, and showing (**a**) the inter-residue n.O.e.'s between α-GalNAc H-1 and α-GalNAc H-4 and the α-Gal H-6,6, (**b**) the close proximity of α-GalNAc H-5 and α-Gal O-3, and (**c**) the steric interaction of the α-GalNAc hydroxymethyl groups and the pyruvic acetal carboxylate group.

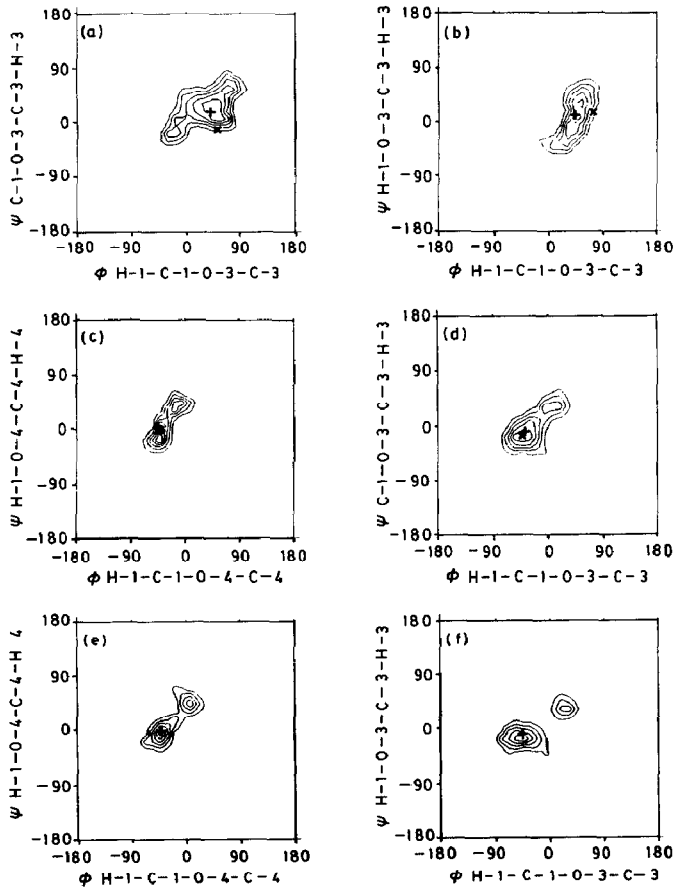

Fig. 8. Van der Waals-energy contour plots for disaccharide fragments of S4 (**1**) and depyruvated S4 (**2**): (a) β-ManNAc-(1→3)-α-FucNAc-OMe, (b) α-FucNAc-(1→3)-α-GalNAc-OMe, (c) α-GalNAc-(1→4)-α-Gal-OMe, (d) α-Gal-(1→3)-β-ManNAc-OMe, (e) α-GalNAc-(1→4)-α-Gal(2,3-pyruvate)-OMe, and (f) α-Gal (2,3-pyruvate)-β-ManNAc-OMe: + time-averaged conformations, × n.m.r.-minimised conformations.

sugar residues were considered initially as rigid systems, and the lowest-energy conformations approximately consistent with the n.O.e. data were found by a grid search about the two glycosidic bonds, C-1–O-x and O-x–C-x, at intervals of 5°. The inter-residue constraints derived from n.O.e.'s are listed in Table VI. Inter-residue inter-proton distances were estimated from $(\text{distance})^{-6}$ comparisons with intra-residue n.O.e.'s and distances. When an inter-residue n.O.e. was not observed, or weak, a lower limit for that inter-proton distance was set at 3 Å, and the minimum permissible inter-proton distance was set at 2.0 Å. Spin diffusion causes the longer inter-proton distances to be underestimated, so that constraints based on large n.O.e.'s (short distances) were given priority. When this grid search was repeated on the decasaccharides, similar values of the glycosidic angle were found. Minimisation of the α-Gal-(1→3)-β-ManNAc linkage is given as an example of this procedure (Fig. 9). Irradiation of the α-Gal H-1 gives an intra-residue n.O.e. of 33% of the H-2 resonance (H-1 to H-2

TABLE VI

N.O.e.-based constraints used to set up the computer model of **4**

	From n.O.e.	*Constraint*	*Found in model*
α-Gal-(1→3)-β-ManNAc			
α-Gal H-1 to β-ManNAc H-3	2.48	2.0 to 2.95	2.49
α-Gal H-1 to β-ManNAc H-4	2.85	2.28 to 3.42	4.92
α-Gal H-1 to β-ManNAc H-2	3.13	2.50 to 3.76	4.30
α-Gal H-1 to β-ManNAc H-5	2.97	2.48 to 3.56	4.48
β-ManNAc H-2 to α-Gal H-4	2.54	2.03 to 3.05	4.81
β-ManNAc H-2 to α-Gal H-5	2.06	2.0 to 2.47	2.30
β-ManNAc-(1→3)-α-FucNAc			
β-ManNAc H-1 to α-FucNAc H-3[a]	2.20	2.0 to 2.64	2.41
β-ManNAc H-1 to α-FucNAc H-4	3.01	2.40 to 3.60	2.61
β-ManNAc H-5 to α-FucNAc H-3	3.12	2.50 to 3.74	3.52
α-FucNAc-(1→3)-α-GalNAc			
α-FucNAc H-1 to α-GalNAc H-3	2.97	2.38 to 3.56	2.23
α-FucNAc H-1 to α-GalNAc H-4	3.80	3.04 to 4.56	3.64
α-GalNAc-(1→4)-α-Gal			
α-GalNAc H-1 to α4-Gal H-4[b]	2.44	2.00 to 2.93	2.20
α-GalNAc H-1 to α-Gal H-1	2.71	2.17 to 3.25	6.03
α-GalNAc H-1 to α-Gal H-3	2.85	2.28 to 3.42	4.53

[a] Referenced to ManNAc H-1 to H-5 as 2.368 Å, 38% n.O.e.; referenced to ManNAc H-5 to H-4 as 3.120 Å, 15% n.O.e. [b] Referenced to α-GalNAc H-1 to H-2 as 2.47 Å, 33% n.O.e., and taken from the α-Gal residue as the α-GalNAc H-2 is under the water signal.

2.47 Å), and an inter-residue n.O.e. of 34% of the β-ManNAc H-3 resonance. A simple ratio of (inter-proton distance)^6 gives an estimate of Gal H-1 to ManNAc H-3 distance of 2.46 Å. When modelling this bond, only conformations in which the Gal H-1–ManNAc H-3 distance was 2.46 Å ± 20% (2.00 to 2.95 Å) were considered further. Similarly, the observed 21% n.O.e. of the Gal H-5 resonance on pre-irradiation of

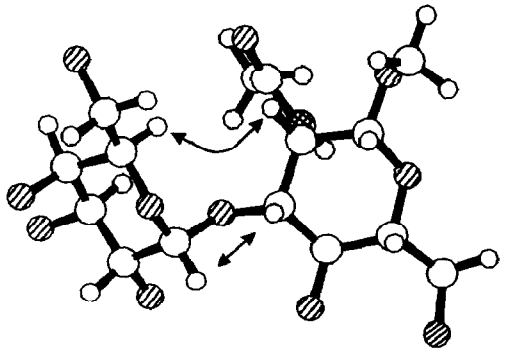

Fig. 9. Conformation of α-Gal-(1→3)-β-ManNAc-OMe, in the conformation found in the n.m.r.-minimised decasaccharide. The arrows show the two inter-residue n.O.e.'s used to determine the conformation.

ManNAc H-2 (compared to a 7% n.O.e. of the ManNAc H-1 resonance at a distance of 2.47 Å) gave an estimated inter-proton distance of 2.06 Å, and only conformations with that distance in the range 2.00–2.47 Å were considered further. The grid search was then performed and the energy was calculated only for those conformations that satisfied the n.O.e. constraints and using a non-bonding potential to estimate the energies. This structure was minimised further by allowing rotation of all pendant groups and glycosidic bonds, using the non-bonded potential in order to produce the "v.d.W.-minimised conformation" for the decasaccharide derivatives **4** and **5**.

French[33] commented that distortion of the sugar ring can influence the preferred conformations of oligosaccharides and an attempt to model this effect was made. A series of overlapping trisaccharide methyl glycosides was constructed with initial values of the glycosidic angles set as derived above, and these model systems were minimised using the MM2CARB program (our version of MM2 has an upper limit of 100 atoms). From these trisaccharide glycosides, two decasaccharide glycosides (pyruvated and depyruvated) were reconstructed as shown below.

```
ManNAc-FucNAc-GalNAc-Gal-ManNAc-FucNAc-GalNAc-Gal-ManNAC-FucNAc-

[A------B----]-C          A----[-B----]-C

       B----[-C---]-D           B----[-C---]-D

            C---[-D---]-E            C---[-D---]-E

                 D---[-E---]-F            D---[-E-----F-OMe]
```

This stage of the minimisation gave rise to the "MM2-minimised conformation", and the glycosidic angles were similar to those in the "v.d.W-minimised conformation". The "MM2-minimised" structure for **5** is shown in Fig. 10.

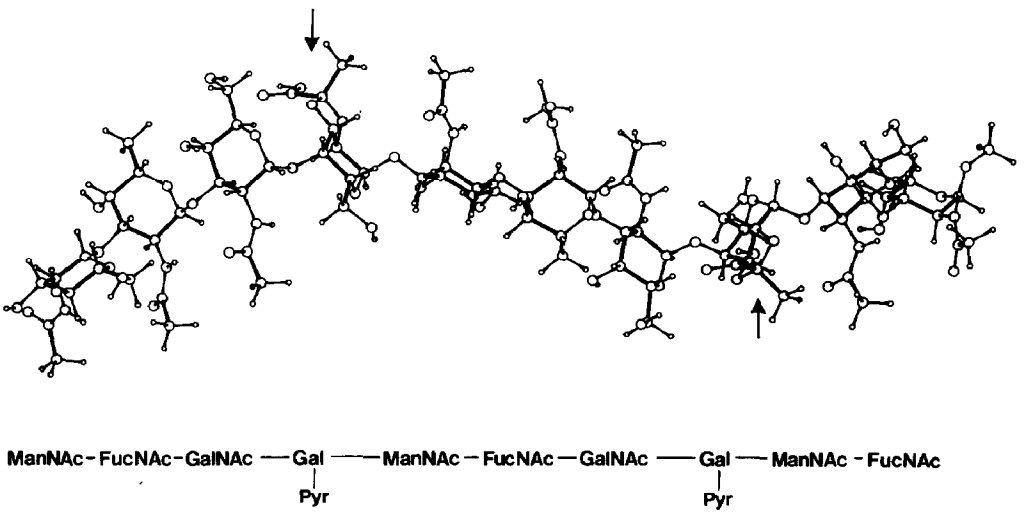

Fig. 10. Computer model of the "MM2-minimised conformation" of the pyruvated polysaccharide **5**. The locations of the pyruvic acetal groups are indicated by arrows.

Adjustment of the computer model to fit the n.m.r. data. — The MM2-minimised structure was used for a complete simulation of the n.O.e.'s, using a model which accounts for multispin effects, fast free rotation of methyl groups, and spin diffusion[22]. A single correlation time of 10 ns was estimated by fitting the α-Gal H-1 to H-2 intra-residue n.O.e. The fit between observed and simulated n.O.e.'s (or, in early experiments, cross-relaxation rates) was improved by adjusting the structure, whilst taking into account short proton–oxygen distances (see below). This process was repeated until there was an acceptable fit between experimental and simulated n.O.e.'s, and was done both manually and by using a Monte Carlo algorithm programmed into NOEMOL.

For the α-FucNAc-(1→3)-α-GalNAc linkage, the lowest-energy conformation was found to be at variance with the original n.O.e. constraints, and the use of this structure in the n.O.e. simulation experiments (see below) gave poor agreement with the experimental data. The observed n.O.e. (13%) is small compared to other n.O.e.'s across the glycosidic linkage. The energy-minimised models also predicted two short inter-residue C–···O– distances (α-FucNAc H-5–α-GalNAc O-4 and α-GalNAc H-4–α-FucNAc O-5). Bock *et al.*[31] have used the deshielding associated with an oxygen atom in close proximity to define particular conformations, but large downfield shifts on FucNAc H-5 and GalNAc H-4 (compared to model systems) were not apparent. Adjustment of this linkage to optimise the fit between experimental and simulated cross-relaxation rates, whilst avoiding short proton–oxygen distances, resulted in a significant change in the glycosidic angles from those in the energy-minimised models, but a far superior fit to the experimental data.

For the α-Gal-(1→3)-β-ManNAc linkage, the simulations suggested that the α-Gal H-1–β-ManNAc H-5 distance in the model is slightly too long (or is in fast equilibrium with a conformer with a very short α-Gal H-1–β-ManNAc H-3 distance). Similarly, the α-Gal H-5–β-ManNAc H-2 distance was found to be too short in the model to fit the experimental data.

Application of this n.O.e. method to the α-GalNAc-(1→4)-α-Gal linkage, where n.O.e.'s are observed between the GalNAc H-1 and the Gal H-4,6,6, is complicated by the extra degree of freedom about the Gal C-5–C-6 bond and the equivalence of the two Gal H-6 resonances. Attempted adjustment of this glycosidic linkage by the n.O.e. method produced a structure with an unacceptably short (2.15 Å) GalNAc H-5–Gal O-3 distance, and the energy-minimised geometry for this glycosidic link was retained.

This decasaccharide structure is referred to as the "n.m.r.-minimised conformation". The glycosidic angles found in these three structures are compared in Table VII. Experimental and simulated n.O.e.'s for the n.m.r.-minimised model are tabulated in Table V.

Relaxation studies and justification of the isotropic tumbling model. — The simulation of inter-proton n.O.e.'s and other relaxation processes is closely linked with the determination (or assumption) of a model for the motions of the molecule. A rigid molecule tumbling isotropically, with no internal motion faster than that of tumbling, is usually assumed. This model requires the determination of a single correlation time, and may be refined easily to allow for fast free rotation of methyl groups.

TABLE VII

Comparison of glycosidic angles in v.d.W.-[a] and MM2-minimised structures

Glycosidic angle	**4**					**5**		
	v.d.W.	*Time-averaged*		*MM2*	*N.m.r.*	*MM2*	*Time-averaged*	
		70°	*20°*				*70°*	*20°*
ManNAc-(1→3)-FucNAc								
H-1–C-1–O-3–C-3	58	40.5	40.3	54	52	52	40.5	40.3
C-1–O-3–C-3–H-3	3	15.7	14.2	16	−11	16	15.7	14.2
FucNAc-(1→3)-GalNAc								
H-1–C-1–O-3–C-3	47	42.6	43.3	52	77	53	43.5	43.3
C-1–O-3–C-3–H-3	7	10.0	10.0	−25	12	−22	10.0	10.0
GalNAc-(1→4)-Gal								
H-1–C-1–O-4–C-4	−42	−41.0	−41.8	−42	−42	−43	−39.4	−40.3
C-1–O-4–C-4–H-4	−8	−2.2	−3.5	−1	−1	−16	−0.2	−1.1
Gal-(1→3)-ManNAc								
H-1–C-1–O-3–C-3	−48	−39.1	−40.6	−54	−44	−55	−50.5	−51.8
C-1–O-3–C-3–H-3	−15	−13.8	−15.0	−20	−17	−21	−10.8	−11.1

[a] Van der Waals.

We have shown[22,34] for *N*-desulphated *N*-reacetylated heparin that a symmetric top model, with relatively slow tumbling perpendicular to the major axis and faster rotation about that axis, best explains the ^{1}H and ^{13}C relaxation data. In this motional model, the relaxation rates depend on the inter-nuclear distance and the angle that the vector (the H···H vector for n.O.e.'s and the C–H bond for carbon T_1s) makes with the major axis. Two correlation times and the major axis must be determined.

More complex models are possible, but more experimental data would be required in order to define the additional parameters.

Longitudinal relaxation in bacterial high-molecular-weight polysaccharides is dominated by internal motions that are difficult to define. Fast motions (compared to the correlation time), such as rotation of the methyl group, and slow motions (such as conformational exchanges) can be accounted for readily[35], but motions with correlation times of the same order as overall reorientation cannot be accounted for at present, and uncorrelated motions of approximately this frequency can lead to significant errors in the n.m.r.-determined conformation[36,37]. N.O.e. simulation based on calculated molecular dynamics trajectories are, computationally, too intensive for motions on this time scale. Measurements of R_1 and R_2 for ^{13}C were carried out in order to define these motions more precisely. The R_1 rates for the methine carbons are similar, with relaxation rates ranging from 3.5 to 2.6 s^{-1} in S4 and from 2.8 to 3.3 s^{-1} in the depyruvated S4. When the angle between the C–H vector of the methine carbons and the major axis (determined as the principal moment of inertia of the decasaccharide and effectively the long axis of the helix) was determined from the computer models and plotted against the experimental relaxation rates, no significant correlation and no evidence for the symmetric top model were found. Similarly, no significant relationship between the intra-residue inter-proton n.O.e.'s and the angle between the inter-proton vector and the major axis was found, and thus the simplest motional model, namely, isotropic tumbling, was used. However, the caveats about the influence of internal motion must be emphasised, and the correlation used for n.O.e. simulations is an "effective" correlation time.

Computer models. — Both the energy-minimised and n.m.r. models are essentially helical, although the latter is more elongated. The helical rise for the energy-minimised model is 16.3 Å, compared with 16.5 Å for the n.m.r. model. MM2CARB energy minimisation tended to push the H-2–C-2–N–H linkage out of planarity and these interactions were relieved in the n.m.r. model. In the n.m.r.-minimised model, FucNAc H-3 was found to be close (2.68 Å) to β-ManNAc O-5, which explains its low-field resonance relative to that of α-GalNAc H-3.

Effect of pyruvic substitution on the conformation of the repeating unit. — The relatively small differences in ^{1}H and ^{13}C chemical shifts between S4 and depyruvated S4 suggested that any changes in conformation due to the presence of the pyruvic moiety were likely to be local, and probably restricted to the α-GalNAc-(1→4)-α-Gal and α-Gal-(1→3)-β-ManNAc linkages. Two specific probes of the glycosidic angles of these bonds are available, namely, the chemical shift of the α-GalNAc H-5 resonance and the β-ManNAc H-2–α-Gal H-5 n.O.e.

The GalNAc H-5 resonates at 4.40 p.p.m. in depyruvated S4, which is moved downfield from 4.14 p.p.m. in the tetrasaccharide derivative **3a** by the proximity of α-Gal O-3. In S4, this resonance is found at 4.29 p.p.m., which implies an increase of this proton–oxygen distance. This finding is consistent with the results of molecular modelling, where the GalNAc H-5–Gal O-3 distance increased from 2.36 to 2.59 Å in the minimum-energy conformations with the introduction of the pyruvic acetal, due mainly to a change of 15° in the C-1–O-4–C-4–H-4 dihedral angle. This change was also reflected in the time-averaged conformations (see below). This analysis is complicated by substitution of the Gal O-3, which reduces its electronegativity[31]. The driving force for this conformational change appears to be a reduction of the non-bonded interactions of the carboxylate and GalNAc hydroxymethyl groups. This effect rationalises the change in chemical shift and unusual temperature dependence of the GalNAc C-6 resonance (see below), and the relaxation rate data are consistent with a change in the conformational space available to the hydroxymethyl group in the S4.

The strong inter-residue n.O.e. between α-Gal H-5 and β-ManNAc H-2 was present in both polysaccharides **1** and **2**, but spectral overlap and differences in the correlation times made quantitation impossible. The molecular modelling showed no significant difference in the glycosidic linkage between the energy-minimised conformation in **4** and **5**, as reflected in the time-averaged structure.

Effect of pyruvation on the dynamics. — The broader lines in the 1D ^{1}H-n.m.r. spectra and faster build-up of spin diffusion during n.O.e. experiments in S4 (compared to the depyruvated S4) was consistent with higher spin–spin relaxation rates (*i.e.*, slower internal motions/overall tumbling) for S4, and this view accorded with the ^{13}C T_2 measurements. The ^{13}C T_1 measurements, however, are anomalous, with little change between S4 and depyruvated S4. As the overall conformation of the two polysaccharides seems to be similar, and with only the GalNAc-(1→4)-Gal linkage significantly more constrained by pyruvation, the effect appears to arise from the hydration associated with the carboxylate group.

Internal motions. — The early work of Lemieux *et al.*[38], using n.m.r. data and HSEA energy calculations, suggested that glycosidic linkages generally existed in a single deep-energy well, and that only a single conformation need be considered, whereas more recent work on small oligosaccharides has suggested that a conformational equilibrium exists between multiple, discrete, energy minima at room temperature[39–43]. Molecular dynamics simulations of a constrained cyclic system, cyclomaltohexaose (α-cyclodextrin) in a water box[44], showed that, during the time-span of the simulation, only a single energy well for the glycosidic linkage was populated, but that the plane of the sugar ring "wobbled" by ±15° about the mean position, and that the hydroxymethyl groups were more flexible.

A knowledge of the contours of the energy surface allows the calculation of time-averaged properties, a technique that has recently been applied to $^3J_{C,H}$ across the glycosidic linkage[41] in a disaccharide and inter-residue n.O.e.'s[45,46], although the theoretical model[47] and simulations[36] indicate that, when the motions are of a similar frequency

to the correlation time, the magnitude of the n.O.e. depends on the inter-proton distance and the re-orientation of the inter-proton vector in the laboratory frame.

We have applied a similar technique, calculating time-averaged conformational data at two temperatures, using conformational maps generated from v.d.W. energy calculations and application of the Boltzmann equation, to explain the variable-temperature n.m.r. data and to show that they are consistent with the proposed conformation.

The narrow spectral lines observed for such high-molecular-weight polysaccharides suggest that relaxation is dominated by internal motions, but the "wobble" of residues within a single energy minima may not be sufficient to explain this effect and an explanation based on a conformational equilibrium is required. Computer simulations to investigate this are in progress.

N.O.e.'s. — Quantitative interpretation of cross-relaxation rates is complicated by the changes in correlation time that occur with temperature, and these data were not collected. The relatively clean effects observed at 70°, and the absence of significant observed n.O.e.'s not predicted by the single conformation model, suggest the presence of only one major conformation.

Variable-temperature ^{13}C data. — The ^{13}C chemical shift data for S4 (**1**), depyruvated S4 (**2**), and the tetrasaccharide derivative (**3a**) vary linearly with temperature over the range 27–77°, and are incompatible with a phenomenon such as gelling. The largest changes were observed for the β-ManNAc C-1 resonance and the glycosylated positions, with differences of up to 0.56 p.p.m. over a temperature range of 40°.

Several studies have related changes in chemical shift with changes in conformation around glycosidic linkages. These changes can be large, for example Saitô *et al.*[47] found conformationally dependent changes in the chemical shift of linkage carbons of up to 6 p.p.m., although the changes in the glycosidic angles were not quantified. Veregin *et al.*[48], working in the (1→4)-α-D-glucan series, correlated ^{13}C chemical shifts with the glycosidic angles, C-1 with the dihedral angle about the O-4–C-4 linkage, and C-4 with the dihedral angle about the C-1–O-4 linkage. Gidley and Bociek[49] confirmed this correlation for the chemical shift of the C-1 resonance, but not for that of the C-4 resonance, and others[50,51] have applied this idea with similar conclusions. In general, a change of 10° in a dihedral angle causes a change of 1–2 p.p.m. in the chemical shift of the C-1 resonance and a change of 1–6 p.p.m. in that of the C-x resonance. If the magnitude of these correlations is valid for the linkages found in the depyruvated S4, time-averaged dihedral angles for the glycosidic bonds change by $<5°$ over a temperature range of 40°. Calculations based on the van der Waals energies show that the magnitudes of time-averaged changes in the glycosidic angles vary between 0.0 and 1.5° between 20° and 70°, in reasonable agreement within the limitations of the force field used. Other ^{13}C chemical shift correlations based on the interactions of protons have been published[50,52].

The single resonance for the hydroxymethyl group arises from fast averaging of the possible rotamers, and the chemical shifts for the resonances of the hydroxymethyl group in these "pure" rotamers have been estimated in the *gluco* series by Horii *et al.*[51],

and differ by ~5 p.p.m. The change in sign of the temperature coefficient of the α-GalNAc C-6 resonance can be explained by a change in the relative stability of, probably, the *gt* and *tg* forms in S4 and depyruvated S4.

Variable-temperature ^{1}H-n.m.r. data. — The model discussed above predicts several short, inter-residue proton–oxygen distances, and a change in these time-averaged distances with temperature should be reflected in relatively large changes in the chemical shifts of the ^{1}H resonances with temperature. The ^{1}H-n.m.r. spectrum of the depyruvated S4 was assigned at 20° from the double-quantum-filtered COSY spectrum. Only one large (>0.05 p.p.m.) change was observed, for the α-GalNAc H-5 resonance, which implied a shortening of the GalNAc H-5–Gal O-3 distance with decreasing temperature. This finding accords with a shortening of the time-averaged inter-nuclear distance from 2.782 Å at 70° to 2.738 Å at 20°. Other, smaller changes (0.02–0.03 p.p.m.) were associated with the glycosidic linkages (ManNAc H-1, ManNAc H-3, FucNAc H-3, GalNAc H-3, and Gal H-4).

Thus, the lowest energy conformations consistent with the n.m.r. data are similar for S4 and depyruvated S4, with the *N*-acetyl groups on adjacent residues projecting on the same side, and the pyruvic acetal projecting away from the main chain (Fig. 10). The presence of the pyruvic acetal has only minor effects on local and overall conformation of the chain, or on local mobility, except that the GalNAc hydroxymethyl group is sterically hindered in the pyruvated polymer, but results in considerable changes in the slower motions, as estimated from ^{13}C R_2 measurements.

The n.m.r. data predicted a structure more similar to the time-averaged conformation than to the energy-minimised structures. The structures determined from n.m.r. measurements at 70° differed little, and in a predictable manner from those present at lower, more physiologically relevant temperatures.

ACKNOWLEDGMENTS

We thank the M.R.C. for access to the M.R.C. Biomedical NMR Centre (Mill Hill), and Drs. Tom Frenkiel and Chris Bauer for help with the spectrometers, Miss Maria Cody for the h.p.l.c., and Merck, Sharp and Dohme Ltd. for the gift of the S4.

REFERENCES

1 J. B. Robbins, R. Austrian, C. J. Lee, S. C. Rastogi, G. Schiffman, J. Hendricksen, P. H. Makela, C. V. Broome, R. R. Facklam, R. H. Tiesjema, and J. C. Parke, *J. Infect. Dis.*, 148 (1983) 1136–1159.
2 (*a*) P.-E. Jansson, B. Lindberg, and U. Lindquist, *Carbohydr. Res.*, 95 (1981) 73–80; (*b*) C. Jones and F. Currie, *ibid.*, 184 (1988) 279–284; (*c*) C. Jones, *ibid.*, 198 (1990) 353–357.
3 G. J. Gerwig, J. P. Kamerling, and J. F. G. Vliegenthart, *Carbohydr. Res.*, 77 (1979) 1–7.
4 C. Erbing, L. Kenne, B. Lindberg, J. Lönngren, and I. W. Sutherland, *Carbohydr. Res.*, 50 (1976) 115–120; G. G. S. Dutton and A. V. Savage, *ibid.*, 84 (1980) 297–305; P.-E. Jansson, B. Lindberg, and G. Widmalm, *ibid.*, 182 (1988) 166–168.
5 I. J. Goldstein, G. W. Hay, B. A. Lewis, and F. Smith, *Methods Carbohydr. Chem.*, 5 (1965) 361–370.
6 I. Tsaroska and T. Bleha, *Adv. Carbohydr. Chem. Biochem.*, 47 (1989) 45–123.
7 C. Jones, B. Mulloy, A. Wilson, A. Dell, and J. E. Oates, *J. Chem. Soc., Perkin Trans. 1*, (1985) 1665–1673.
8 S. C. Szu, G. Zon, R. Schneerson, and J. B. Robbins, *Carbohydr. Res.*, 152 (1986) 7–20.

9 W. M. Blanken, M. L. E. Burgh, P. L. Koppen, and D. H. van den Eijnden, *Anal. Biochem.*, 145 (1985) 322–330.
10 W. P. Aue, E. Bartholdi, and R. R. Ernst, *J. Chem. Phys.*, 64 (1976) 2229–2246; K. Nagayama, A. Kumar, K. Wuthrich, and R. R. Ernst, *J. Magn. Reson.*, 40 (1980) 321–334.
11 G. Bodenhausen, H. Kogler, and R. R. Ernst, *J. Magn. Reson.*, 58 (1984) 370–388.
12 D. Neuhaus and M. Williamson, *The Nuclear Overhauser Effect in Structural and Conformational Analysis*, Verlag Chemie, New York, 1989, p. 105.
13 P. J. Hore, *J. Magn. Reson.*, 55 (1983) 283–300.
14 A. Bax and G. Morris, *J. Magn. Reson.*, 42 (1981) 501–505.
15 H. Kessler, C. Griesenger, J. Zarbock, and H. R. Loosi, *J. Magn. Reson.*, 57 (1984) 331–336.
16 (*a*) W. F. Reynolds, D. W. Hughes, M. Perpick-Dumont, and R. G. Enriquez, *J. Magn. Reson.*, 64 (1985) 304–311; (*b*) G. H. Cockin, T. N. Huckerby, and I. A. Nieduszynski, *Biochem. J.*, 236 (1986) 921–924.
17 E. L. Hahn, *Phys. Rev.*, 80 (1950) 580–594; H. Y. Carr and E. M. Purcell, *ibid.*, 94 (1954) 630–639.
18 E. L. Hahn, *Phys. Rev.*, 77 (1950) 297–298.
19 J. Gasteiger and M. Marsili, *Tetrahedron*, 36 (1980) 3219–3228.
20 N. L. Allinger and Y. H. Yuh, *QCPE*, 13 (1981) 395.
21 G. A. Jeffrey and R. Taylor, *J. Comput. Chem.*, 1 (1980) 99–109.
22 M. J. Forster, C. Jones, and B. Mulloy, *J. Mol. Graphics*, 7 (1989) 196–201.
23 H. M. Berman, *Acta Crystallogr., Sect. B*, 26 (1970) 290–299.
24 H. J. Jennings, C. Lugowski, and N. M. Young, *Biochemistry*, 19 (1980) 4712–4719.
25 H. Ohri, Y. Nishida, H. Higuchi, H. Hori, and H. Meguro, *Can. J. Chem.*, 65 (1987) 1145–1153; Y. Nishida, H. Hori, H. Ohrui, and H. Meguro, *Carbohydr. Res.*, 170 (1987) 106–111.
26 O. Jardetsky and G. C. K. Roberts, *NMR in Molecular Biology*, Academic Press, New York, 1981, p. 158.
27 N. J. Maeji, Y. Inoue, and R. Chujo, *Carbohydr. Res.*, 162 (1987) c4–c7; C. A. Bush and R. E. Feeney, *Int. J. Pept. Protein Res.*, 28 (1986) 386–397.
28 K. Bock and C. Pedersen, *Adv. Carbohydr. Chem. Biochem.*, 41 (1983) 27–66; K. Bock, C. Pedersen, and H. Pedersen, *ibid.*, 42 (1984) 193–225.
29 F. Michon, J.-R. Brisson, and H. J. Jennings, *Biochemistry*, 26 (1987) 8399–8405.
30 L. H. Zhang, M. R. Laughlin, D. L. Rothman, and R. G. Shulman, *Biochemistry*, 29 (1990) 6815–6820.
31 K. Bock, M. Meldal, D. R. Bundle, T. Iversen, B. M. Pinto, P. J. Garegg, I. Kvanström, T. Norberg, A. A. Lindberg, and S. B. Svenson, *Carbohydr. Res.*, 130 (1984) 35–53.
32 Cambridge Structural Database, Cambridge Crystallographic Data Centre, Cambridge.
33 A. D. French, *Biopolymers*, 27 (1988) 1519–1526.
34 B. Mulloy, M. J. Forster, C. Jones, and D. B. Davies, unpublished data.
35 J. Tropp, *J. Chem. Phys.*, 72 (1980) 6035–6043.
36 D. Genest, *Biopolymers*, 28 (1989) 1903–1911.
37 D. Genest and J. P. Simone, *Magn. Reson. Chem.*, 28 (1990) 21–26.
38 H. Thogersen, R. U. Lemieux, K. Bock, and B. Meyer, *Can. J. Chem.*, 60 (1982) 44–57.
39 G. M. Lipkind, A. S. Shashkov, and N. K. Kochetkov, *Carbohydr. Res.*, 141 (1985) 191–197.
40 A. S. Shashkov, G. M. Lipkind, and N. K. Kochetkov, *Carbohydr. Res.*, 147 (1986) 175–182.
41 M. Hricovini, I. Tvaroska, and T. Peters, *Carbohydr. Res.*, 198 (1990) 193–203.
42 S. W. Homans, *Biochemistry*, 29 (1990) 9110–9118.
43 A. Imberty, V. Trau, and S. Perez, *J. Comput. Chem.*, 11 (1990) 205–215.
44 J. E. Koehler, W. Saenger, and W. F. van Gunsteren, *J. Mol. Biol.*, 203 (1988) 241–250.
45 K. Bock, H. Lönn, and T. Peters, *Carbohydr. Res.*, 198 (1990) 375–380.
46 J.-R. Brisson and J. P. Carver, *Biochemistry*, 22 (1983) 3671–3680 and 3680–3686.
47 H. Saitô, R. Tabeta, M. Yokoi, and T. Erata, *Bull. Chem. Soc. Jpn.*, 60 (1987) 4259–4266; H. Saitô, M. Yokoi, and Y. Yoshioka, *Macromolecules*, 22 (1989) 3892–3898; H. Saitô, R. Tabeta, and K. Ogawa, *ibid.*, 20 (1987) 2424–2430.
48 R. P. Veregin, C. A. Fyfe, R. H. Marchessault, and M. G. Taylor, *Carbohydr. Res.*, 160 (1987) 41–56.
49 M. J. Gidley and S. M. Bociek, *J. Am. Chem. Soc.*, 110 (1988) 3820–3829.
50 K. Bock, A. Brignole, and B. W. Sigurskjold, *J. Chem. Soc., Perkin Trans. 2*, (1986) 1711–1713.
51 F. Horii, A. Hirai, and R. Kitamaru, *ACS Symp. Ser.*, 260 (1984) 27–42.
52 N. K. Kochetkov, O. S. Chizhov, and A. S. Shashkov, *Carbohydr. Res.*, 133 (1984) 173–185.